

NUCLEAR STRUCTURE -- THEORY

K. Nakayama, S. Drozd^a, S. Krewald^b, and J. Speth^b

Relativistic dynamical effect is now a subject of considerable interest and discussion in nuclear structure problems. Due to the decoupling of the scalar field in the nuclear interior, this effect introduces an extra density dependence on the effective interaction.¹ Within the conventional Brueckner theory one cannot reproduce the empirical values of the binding energy and saturation point of nuclear matter. The additional density dependence due to the relativistic dynamics, however, tends to cure this problem. Although there are still many serious questions open, relativistic dynamical effects seem to help us in explaining conveniently not only the bulk properties of nuclear matter but also nucleon-nucleus scattering data, especially the spin-observables such as analyzing power and spin rotation probabilities.² Therefore, it is also very interesting to investigate how these effects affect the excited states of nuclei. The present work is devoted to this purpose.

In order to investigate these effects a quasiparticle relativistic G-matrix interaction has been constructed by solving a three-dimensional integral equation obtained from the Bethe-Salpeter equation and compared to the conventional non-relativistic G-matrix interaction. Fig. 1 shows a comparison between these two G-matrices. They are expressed in the spin-isospin transfer representation

$$G = F + F' \vec{\tau}_1 \cdot \vec{\tau}_2 + G \vec{\sigma}_1 \cdot \vec{\sigma}_2 + G' \vec{\sigma}_1 \cdot \vec{\sigma}_2 \vec{\tau}_1 \cdot \vec{\tau}_2 + \dots$$

As one sees, the relativistic effect makes the scalar-isoscalar (F) channel of the interaction much less attractive compared to the non-relativistic case. It reduces the magnitude by a factor -2 in the low momentum transfer region. The other channels including also the tensor

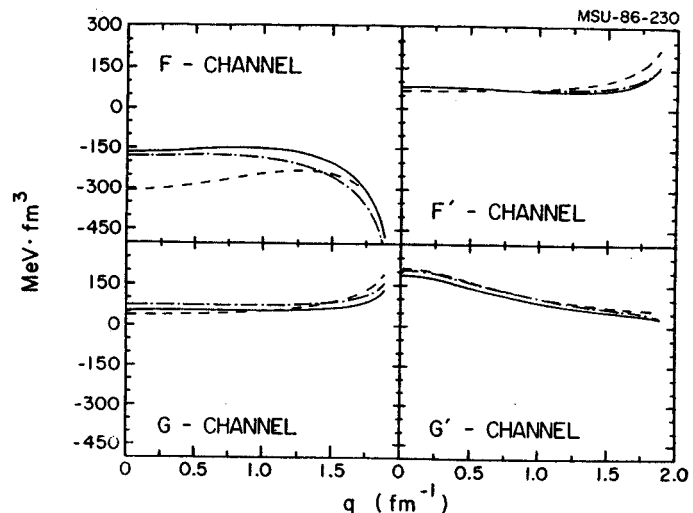


Fig. 1 Central components of the relativistic G-matrix interaction at $k_F = 1.36 \text{ fm}^{-1}$ as a function of momentum transfer. The solid lines correspond to the results using the HM3A version⁵ of the one-boson-exchange potential, while the dash-dotted ones correspond to the BMR2 version.⁶ The dashed curves are the non-relativistic G-matrix of Ref. 7.

components (not shown here) remain basically unaffected. Although the spin-orbit components are not shown, they become much more attractive (by a factor -2 at nuclear matter normal density) with the inclusion of relativistic effects.

In Fig. 2 the binding energy in nuclear matter as a function of density is shown. This was obtained using the relativistic G-matrix. As has been pointed out by other authors,¹ the relativistic effect moves the saturation point out of the Coester line toward the direction of the empirical value.

The compression modulus κ , which is defined as $\kappa = 9\rho(\partial^2(\rho E_B/A)/\partial\rho^2)$ where ρ denotes the density and E_B/A the binding energy per particle in nuclear matter, can be extracted from the result of Fig. 2. This yields $\kappa = 200 \text{ MeV}$ in comparison to $\kappa = 120 \text{ MeV}$ obtained in the

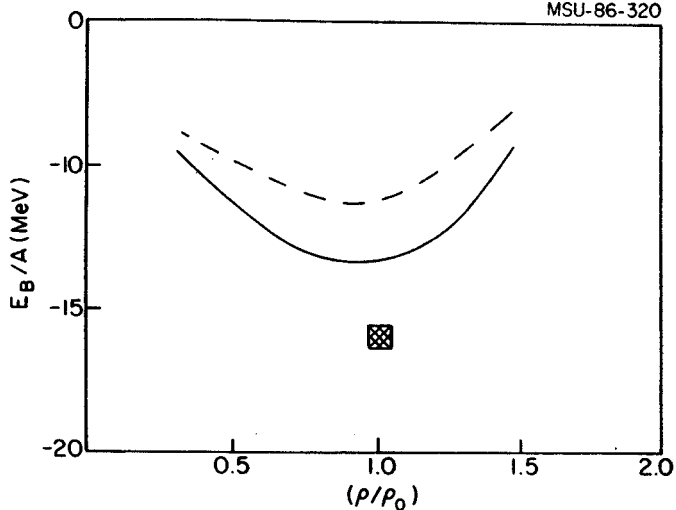


Fig. 2 Binding energy per particle as a function of density in units of $\rho_0 = 0.17 \text{ fm}^{-3}$. The solid curve corresponds to the BRM2 version,⁶ while the dashed curve to the HM3A version⁵ of the one-boson-exchange potential.

corresponding non-relativistic calculation. The empirical value of the compression modulus in nuclear matter is about $\kappa = 230 \text{ MeV}$.

As an example of the application of the relativistic G-matrix as a residual particle-hole interaction, we show in Fig. 3 the results of a RPA calculation of a $J^\pi = 0^+$ state in ^{90}Zr , including 1p-1h as well as 2p-2h configurations. According to the Landau theory, the particle-hole interaction is defined to be the second derivative of the energy functional with respect to the occupation functions. If we use the result of the G-matrix for the ground state energy, the particle-hole interaction is given by³

$$F^{\text{ph}} = G^{\text{ph}} + \text{rearrangement terms}$$

where G^{ph} denotes the particle-hole G-matrix interaction. Rearrangement terms appear due to the density dependence of the G-matrix and the leading term of these contributions is taken into account by including explicitly 2p-2h excitations in the RPA calculation. This leading term can be seen as the lowest order contribution of the induced interaction which

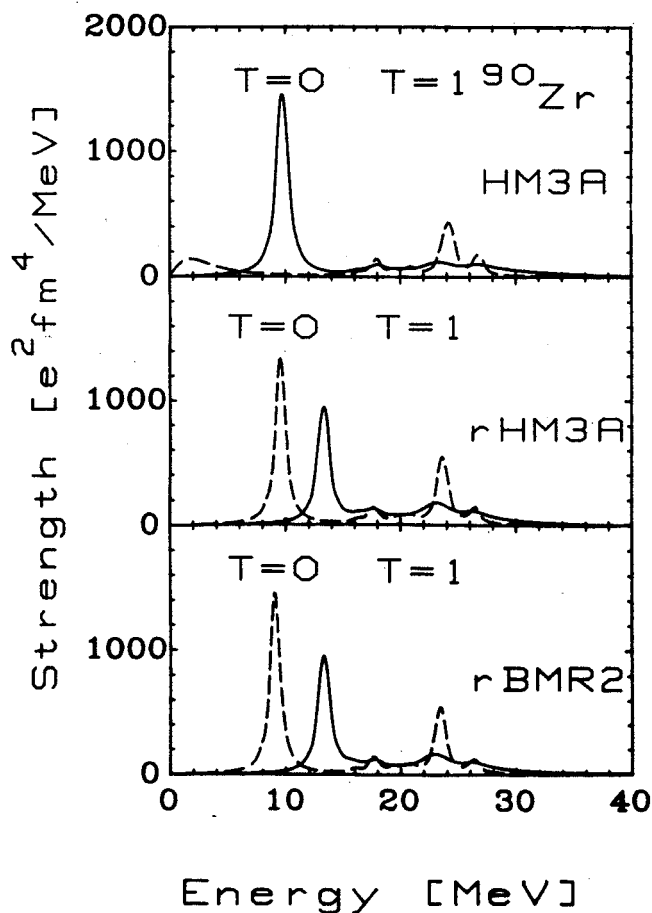


Fig. 3 Strength distribution of the $J^\pi = 0^+$ state in ^{90}Zr . The upper part corresponds to the results obtained using the non-relativistic G-matrix⁷ as the residual interaction, while the middle and lower parts to those of relativistic interactions based on the HM3A⁵ and BMR2⁶ versions of the one-boson-exchange potential, respectively. The solid curves correspond to the RPA results including 2p-2h configurations. The dashed curves are those including only 1p-1h configurations.

arises due to the virtual collective excitation of a nucleus.⁴ In nuclei, the particle-hole interaction is strongly screened by this mechanism. In Fig. 3 the effect of the relativistic dynamics and induced interaction (in lowest order) relative to the non-relativistic G-matrix results is shown separately. As one can see, the latter interaction yields an unstable solution for the breathing (isoscalar $T=0$) mode. Inclusion of 2p-2h excitations cures this instability. In the middle part of Fig. 3 the relativistic G-

matrix result is displayed. Here, one sees that, in contrast to the non-relativistic G-matrix case, the instability problem is no longer observed, which is a consequence of the much weaker F-channel of the interaction as shown in Fig. 1. Inclusion of 2p-2h excitations gives a further repulsion and shifts the breathing mode to much higher excitation energy. The lower part of Fig. 3 is the same as the middle one for a different interaction.

In summary, it seems to be clear that the additional density dependence introduced by using the modified spinors (relativistic effects) helps us to explain also the properties of low-lying excited states of nuclei.

1. M. R. Anastasio, L. S. Celenza, W. S. Pong, and C. M. Shakin, Phys. Rep. 100,327(1983); B. D. Serot and J. D. Walecka, Adv. Nucl. Phys. 16,(1985).
2. M. V. Hynes, A. Picklesimer, P. D. Tandy and R. M. Thaler, Phys. Rev. Lett. 52,978 (1984); Phys. Rev. C31,1438(1985).
3. G. E. Brown, Rev. Mod. Phys. 43,1(1971).
4. S. Babu and G. E. Brown, Ann. Phys. 78,1 (1973).
5. K. Holinde, Phys. Rep. 68,121(1981).
6. R. Machleidt and R. Brockmann; Workshop on "Dirac Approach to Nuclear Physics", LAMPF, Los Alamos, NM, Jan. 31 - Feb. 2, 1985.
7. K. Nakayama, S. Krewald, J. Speth and W. G. Love, Nucl. Phys. A431,419(1984).

-
- a. Institute of Nuclear Physics, Cracow, Poland
 - b. IKP - KFA, Jülich, West Germany

K. Nakayama and G.F. Bertsch

Recently Peterson¹ reported calculations which apparently show that the (α, α') scattering reaction might not be able to distinguish monopole from isovector dipole excitation. Since the monopole is known mainly from this reaction, a mistaken identity due to a masquerading dipole would have serious consequences, particularly for our understanding of nuclear matter compressibility.² We have repeated Peterson's calculations and discover that his findings are not substantiated. The main question is the magnitude and shape of the potential matrix element connecting ground and dipole states. We use Satchler's conventions in defining the deformation parameter of the transition matrix element.³ Then a reasonable approximation to the nuclear potential matrix element is $\langle \text{ex} | U_N(\vec{r}) | 0 \rangle = -\beta_1 R^2 (ZU'_n - NU'_p) Y_1(\hat{r}) / A$, where R is the nuclear radius and U'_n, U'_p are the derivatives of the potentials due to target neutrons and protons. Peterson proposes a similar (but not identical) form. With the phase convention used for the nuclear transition potential here, the Coulomb matrix element is given by $\langle \text{ex} | U_C(\vec{r}) | 0 \rangle = -\beta_1 R^2 N Z e^2 Y_1(\hat{r}) / (r^2 A)$. The magnitude of β_1 is fixed by requiring the dipole state to exhaust the energy-weighted sum rule: $(\beta_1 R)^2 = \pi \hbar^2 A / (2mE_x N Z)$.

We note that Peterson's β_1 has a different magnitude, implying an inconsistency with above transition potentials. We calculated the cross sections for these transition potentials using the code ECIS.⁴ The results are shown in Fig. 1. Both nuclear transition potentials give the expected $L=1$ shape for the angular distribution. In particular, the first minimum is at 5.5° , where the experimental cross section has a maximum. Also, the magnitude of the predicted cross section is small compared to experiment,⁵ and compared to the calculated monopole.⁵ The

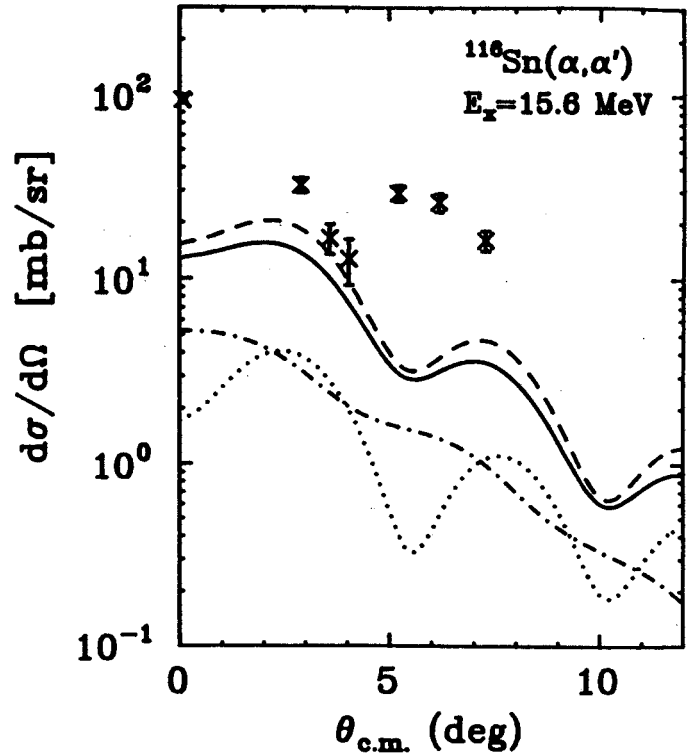


Fig. 1. Comparison between the data from Ref. 5 for the isoscalar monopole excitations at $E_x = 15.6$ MeV in ^{116}Sn with the present calculation of the isovector dipole mode including constructive Coulomb excitation. The solid curve corresponds to the case where the nuclear transition matrix as given in the text has been used, while the dashed curve corresponds to that proposed in Ref. 1 with β_1 as given in the present work. The cross sections for pure Coulomb and pure nuclear excitation are shown as the dash-dotted and dotted curves respectively. Potential parameters were taken from Ref. 5.

argument given in Ref. 1 for an altered phase of large angle oscillations is based on the difference in shape of the dipole transition potential above from the isoscalar transition potential. However, due to strong absorption of the alpha particle in the nuclear surface, one is only sensitive to the far tail of the potential, where shape differences are unimportant.

Finally, for completeness, we show the angular distributions for the Coulomb and nuclear excitation separately. The Coulomb contribution peaks at forward angles and falls rather smoothly at large angles. The interference is constructive with the nuclear contribution.

References

1. R. J. Peterson, Phys. Rev. Lett. 57,1550 (1986).
2. J. P. Blaizot, Phys. Rep. 64,171(1980).
3. G. R. Satchler, Direct Nuclear Reactions, (Oxford, 1983), p. 576.
4. J. Raynal, CEN-Saclay, (unpublished).
5. C. M. Rozsa, et al., Phys. Rev. C21,1252 (1980).

E. Bauer^a, F. Krmpotic^a, and K. Nakayama

In the last few years considerable progress has been made in establishing the properties of giant resonances of both a charge-conserving and charge-exchange nature. It is now possible to evaluate the energy position, the strength and the width of collective states using realistic residual interactions and large 1p-1h as well as 2p-2h configuration spaces. However, these sophisticated calculations do not use a good isospin basis, and therefore do not conserve the isospin symmetry in nuclei with ground state isospin $T_0 = (N-Z)/2 > 0$. It is well known, however, that as a consequence of the conservation of the isospin symmetry, the nuclear spectrum tends to split into states with different isospin quantum number T . A clear manifestation of this phenomenon is the isospin fragmentation of giant resonances. Therefore, we have developed an RPA formalism in which the isospin is treated as a good quantum number. Here, particle-hole states with a definite isospin are decomposed into 1p-1h, 2p-2h and 3p-3h states. It is, however, possible to relate the matrix elements between states with good isospin to the 1p-1h matrix elements with different components of the isospin (not with definite isospin). Moreover, these last quantities can be easily summed up and the final result appears in the form of the matrix element between the usual 1p-1h states, multiplied by a geometrical isospin dependent factor which comes from the 2p-2h and 3p-3h components. The precise relationship between these matrix elements described above is most easily accomplished by using the tensor equation-of-motion method developed in Ref. 1. For details we refer to Ref. 2. As an example of application of the formalism we performed a calculation of the well known Gamow-Teller giant resonances. Experimental data for the energy

splitting between the $T=T_0$ and $T=T_0-1$ components of the Gamow-Teller resonances are available.³ Here, we discuss the double closed nuclei ^{48}Ca and ^{90}Zr . The neutron single-particle states were generated from the Wood-Saxon potential. The single-particle wave functions should be the same for both proton and neutron in the same state i ; then the proton single-particle energy $\epsilon_p(i)$ is related to that of neutron $\epsilon_n(i)$ by $\epsilon_p(i) = \epsilon_n(i) - U_0(i) + \Delta_c$. Here, $U_0(i)$ is the symmetry energy and Δ_c denotes the Coulomb energy displacement including the proton-neutron mass difference. A hamiltonian of the form $H_{\text{res}} = -2\pi(v_s P_s + v_t P_t) \delta(\vec{r}_1 - \vec{r}_2)$ was taken to be the residual interaction, where P_s and P_t are singlet-even and triplet-even projection operators, respectively. When there is a self-consistency between Hartree-Fock field and the collective motion, the symmetry energy is given by

$$U_0(i) = - \sum_j \langle p_i n_j | H_{\text{res}} | p_j n_i \rangle$$

where $\langle ij | H_{\text{res}} | ji \rangle$ is the antisymmetrized proton-neutron matrix element and the sum runs over the neutron excess region.

Table 1 shows the calculated values of excitation energies and transition strengths for $T=T_0-1$ and $T=T_0$ states. For comparison, the results of the standard RPA are also displayed. As one see, the effect of isospin symmetry is to lower the excitation energies. It also causes a quenching of the corresponding transition strengths by transferring a part of them to the states with $T=T_0$. For ^{48}Ca , the excitation energy is decreased by -9% for the higher state. The transition strength is reduced by -7%. For ^{90}Zr , the isospin effect is about 4% for both excitation energy and transition strength. Our results for states with $T=T_0$ are always in the

Table 1

Excitation energies (in MeV) and the transition strengths for the Gamow-Teller transitions. The latter quantities are shown in parentheses. The units is such that the model independent sum rule is $4T_0$. Only the dominant states are displayed. The calculated results with and without good isospin formalism are indicated as theory a) and b), respectively.

Nucleus	Theory a)		Theory b)	Experiment
	$T=T_0-1$	$T=T_0$		
^{48}Ca	1.1(3.5)		1.2(3.8)	2.2(1.2±0.2)
	9.2(11.1)		10.1(11.9)	-10.7(6.0±0.8)
		16.4(1.0)		16.5(0.43±0.0)
^{90}Zr	6.7(3.3)		6.6(4.0)	8.4±0.2(1.2)
	14.7(15.3)		15.3(16.0)	14.8±0.3(5.5)
		21.0(0.93)		19.5±0.4(0.7)

energy region -6-8 MeV above the $T=T_0-1$ states and have very small transition strengths compared to the latter. Although our major aim here is not to compare the present results with the experimental data, the latter are also shown in the table. Bearing in mind that there is no free parameter in the calculation, the agreement between theoretical and experimental energies is quite satisfactory. On the other hand, since we have included no quenching mechanism, such as 2p-2h polarization or Δ -h excitations, the calculated values for transition strengths are always significantly larger than the experiment.

In summary, the RPA formalism with good isospin, as developed here, seems to work well, and therefore its application to the cases where we have smaller T_0 than in the present example seems to be very interesting.

a. University of La Plata, Argentina.

References

1. D. J. Rowe and C. Ngo-Trong, Rev. Mod. Phys. 47, 471(1975).
2. F. Krmpotic, C. P. Malta, K. Nakayama and V. Klemt, Phys. Lett. 149B, 1(1984); E. Bauer, F. Krmpotic and K. Nakayama, to be published.
3. B. D. Anderson, et al., Phys. Rev. Lett. 45, 699(1980); C. Gaarde, et al., unpublished.; D. E. Brainum, et al., Phys. Rev. Lett. 44, 1759(1980); D. J. Horen, et al., Phys. Lett. 95B, 27(1980).

W.T. Chou, W.A. Olivier, Wm. C. McHarris, O. Scholten^a

The IBA model has proven to be able to give a rather accurate description of the properties of low-lying collective levels in even-even nuclei. Likewise, its extension to odd-mass nuclei, the IBFA model, is able to reproduce a large variety of properties in phenomenological calculations. Recently we have developed a computer code¹ with which it is possible to calculate odd-odd nuclei in the framework of the IBA model. We will examine the extension of this model to the odd-odd Re nuclei.

The odd-odd Re nuclei can be considered as coupling a proton hole and a neutron hole to an even-even Os core. The calculation starts from even-even Os cores, to which the odd particles are coupled in the subsequent calculations of the odd-mass nuclei and odd-odd Re nuclei. The states of interest in both the odd-mass and the odd-odd nuclei are primarily based on the lowest levels in the core. Since these are predominantly symmetric in the neutron-proton degree of freedom, a description in terms of the IBA-1 model, where no explicit distinction is made between neutron and proton excitation, is sufficient². We calculate excitation energies and some electromagnetic properties of the cores. All three Os isotopes have a γ band besides the ground-state band. The calculations reproduce the energies of the ground-state bands quite well, while the energies of some members of the γ bands are off. Figure 1 shows the results. The IBA model also gives reasonable estimates of B(E2) transitions; a few important B(E2) transition are shown in Fig. 2.

An odd-mass Re isotope is described in the IBFA model by coupling the degree of freedom of a single proton hole to the even-even Os core. The Hamiltonian of the IBFA can be written as

$$H = H_{IBA} + H_F + V_{BF}.$$

The second term is the Hamiltonian of the fermion, and the third term is the boson-fermion

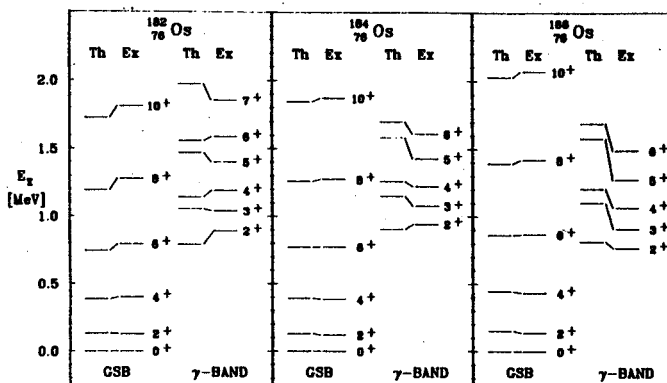


Fig. 1. The calculated excitation energy spectra for the even-even Os isotopes compared with experimental data^{3,4,5}

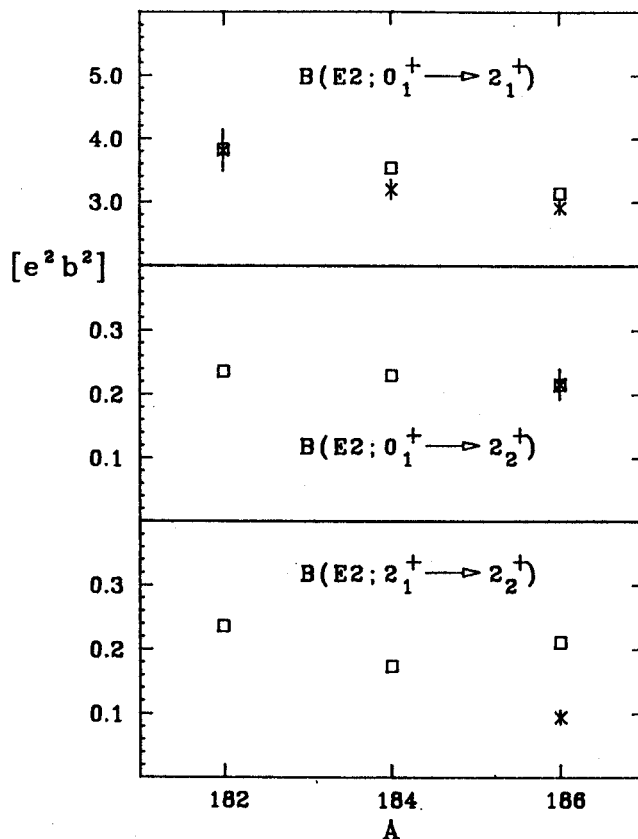


Fig. 2. Some experimental^{6,7} and calculated B(E2) values for the even-even Os isotopes.

interaction. In contrast to other work, where high-spin states and configurations based on unique-parity orbits were studied, in the present work we do not make such a discrimination between the states that are considered. In the description of negative-parity states, not only the $h_{11/2}$ orbit, the unique-parity orbit in the region $Z=50-82$, was considered, but also the $h_{9/2}$ orbit. The reason for including the latter in the calculation is that the state which originates from it was observed experimentally. Since the $h_{9/2}$ orbit was included in the basis, for consistency all positive parity orbits of the 50-82 major shell, $g_{7/2}$, $d_{5/2}$, $d_{3/2}$, and $s_{1/2}$, were included in the calculation, even though the last two have quite high single-particle energies. We calculate the negative-parity states first because they are relatively simple. We can reasonably choose the occupation probabilities, which is one of the parameters describing the boson-fermion interaction. Then we calculate the positive-parity states and use the BCS method to determine the occupation probabilities. The only constraint put on choosing the parameters is that they vary smoothly and systematically from isotope to isotope. An important point to be mentioned is that the occupation probabilities are such that all particles in the 50-82 valence shell are accounted for. Figure 3 is the comparison of excitation energies between calculation and experiment for ^{183}Re ; these serve as the odd-proton part of the odd-odd ^{182}Re states. The positive parity and negative-parity states are plotted separately and relatively to the state of the lowest excitation energy of each parity. Re is in the well-deformed region, and the spectra clearly show rotational behavior. The calculation reproduces the rotational feature quite well. (A $K=1/2$ band is always troublesome in IBFA calculation, and we can only fit the $I+2$ branch well.)

The odd-mass Os isotopes are considered in the IBFA model as a neutron hole coupled to the

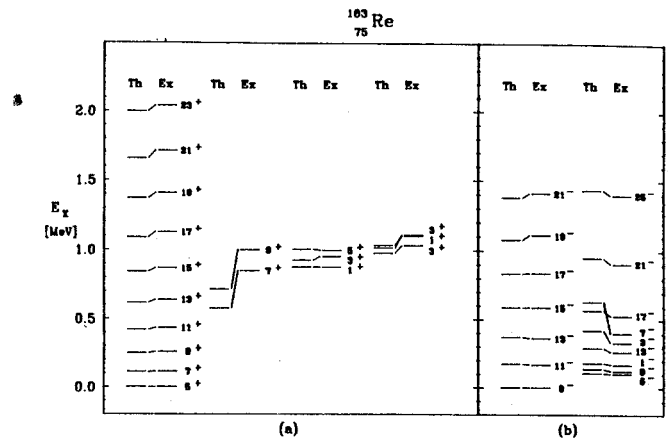


Fig. 3. Calculated and experimental^{8,9} relative energies for $^{183}_{75}\text{Re}$. (a) shows positive parity levels, (b) negative parity levels. The levels are labelled with twice their spin value.

even-even Os core. The same principle was followed as for the calculation of the odd-mass Re isotopes. Because of the ambiguity in the experimental results, and because of five single-particle orbits involved in the negative parity states, no detailed fit of the excitation energies was attempted. The results for ^{183}Os are shown in Figure 4. Only one positive-parity band was observed for ^{183}Os . This band, originating from $i_{13/2}$, is staggered due to the large Coriolis matrix elements. The calculation shows that the $K=1/2^-$ band is a highly staggered band, while the preliminary results of a heavy-ion reaction¹⁰ reported only the $I=K+2$ members. The $3/2^-$ member of this $K=1/2^-$ band was seen in the decay of ^{183}Ir ¹¹ so we think the calculation is acceptable. We also made calculations of electromagnetic moments for these two odd-mass nuclei. The results are compared with experiment values in Table 1.

The structure of odd-odd deformed nuclei is dominated by the features of the coupling of each of the two odd particles to the core. The Hamiltonian can be written as

$$H = H_{\text{IBA}} + H_{n,F} + H_{p,F} + H_{n,BF} + H_{p,BF} + V_{n,p},$$

$$\text{where } V_{n,p} = V_{q,n} \cdot Q_p + V_{s,n} \cdot S_p.$$

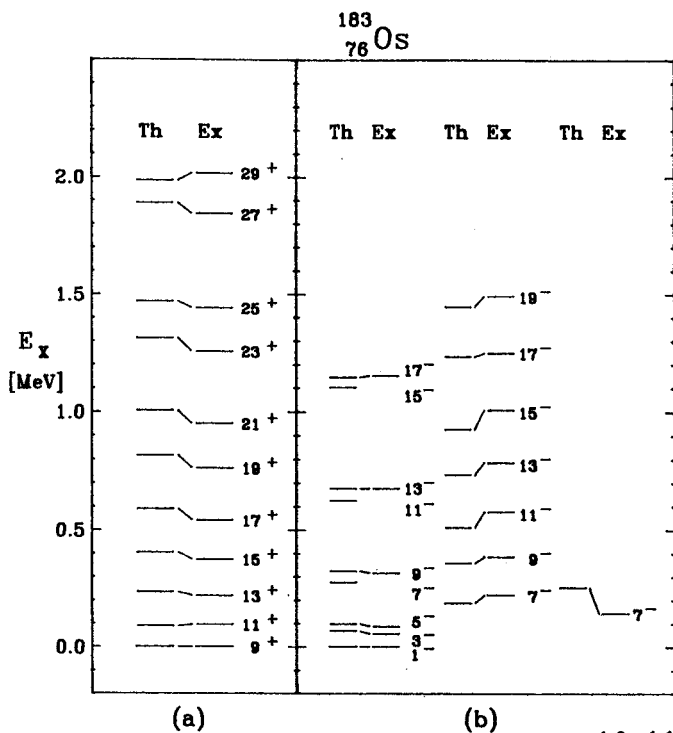


Fig. 4. Calculated and experimental^{10,11} relative energies for the $^{183}_{76}\text{Os}$. (a) is for positive-parity levels; (b) negative parity levels. The levels are labelled with twice their spin value.

Table 1. List of calculated (Th) and experimental (Ex) values of quadrupole moments (Q) and magnetic moments (μ).

	Q		μ	
	Th	Ex	Th	Ex
$^{183}_{75}\text{Re}$	6.36	5.48	2.87	3.17
$^{183}_{76}\text{Os}$	5.44	6.20	1.00	0.782

The first five terms are pre-determined from the previous even-even and odd-mass calculations. The last term is the neutron-proton residual interaction. This residual interaction plays a relatively minor role.¹ The reason lies in the fact that the dominant component of this residual interaction is a quadrupole-quadrupole force and it is already taken into account via the particle-boson interaction in the IBFA calculation. Thus, we set $V_q=0$. Only the spin-spin component of the residual interaction has

been considered. Its effect on the spectrum is that it introduces a splitting in energy of states built on a singlet versus a triplet coupling. In the calculation of the odd-odd Re isotopes, the strength of the spin-spin interaction was chosen to be -0.02 MeV, constant for all orbits and isotopes. This roughly reproduces the spin singlet-triplet coupling observed near closed shells. In the actual calculations, the model space has been truncated. For example, in the calculation of ^{182}Re , the degree of freedom of the odd-proton hole is coupled to the lowest 15 states of each spin and parity of the ^{183}Os odd-neutron core. It has been verified that by decreasing this number to the lowest 12 states, the excitation energies of the levels of interest, results in a difference of less than 10 keV. We also probed the effect of space truncation by coupling an odd-neutron hole to the ^{183}Re odd-proton core, and the states of interest were calculated to within 20 keV of the same energies. The calculated energy spectrum is compared with the available data in Fig. 5. Four rotational bands and a few other states have been fully identified. The 7^+ is the ground state and this 7^+ and the 2^+ are spin triplet versus singlet couplings. Unfortunately we do not know the excitation energy of the 2^+ state. The calculations shows for the $K=2^+$ to be 38.6 keV higher than the $K=7^+$. Thus, we plot the results in two parts in Fig. 5, one with $K=7^+$ as base, the other $K=2^+$. The results, except the $K=4^-$ band, are remarkably good. The $K=4^-$ state, results from the coupling of a $1/2^-$ proton with a $9/2^+$ neutron. Remember we did not fit the $K=1/2^-$ band too well, and we estimated the staggering of the $K=9/2^+$ band. Thus, the result for this 4^- band is not as good as for the others. We do get the right splitting of singlet versus triplet for all of these bands, but it is not always correct for some higher-energy bands.

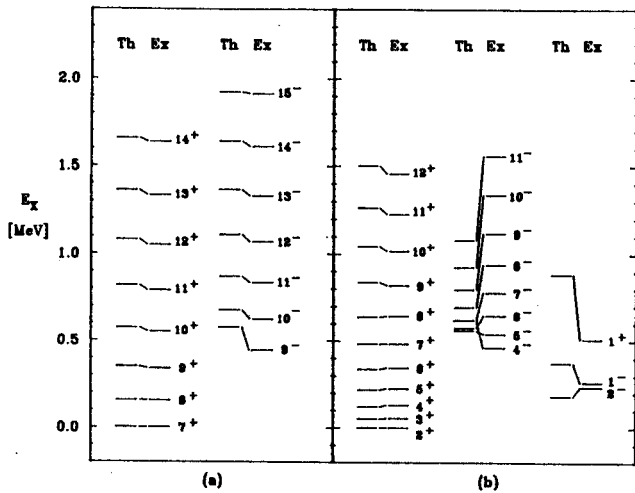


Fig. 5. The calculated excitation energy spectrum for odd-odd $^{182}_{75}\text{Re}$. In (a) all the levels are plotted relative to 7^+ , while in (b) they are plotted relative to 2^+ .

We have also calculated $^{180,184}\text{Re}$, but they are not completely analyzed yet. From the results we have now, we think the IBFFA model works fairly well. If good fits of even-even and odd-mass nuclei can be obtained, then good spacings in odd-odd nuclei are likely. We do not always get the right splitting of singlet versus triplet coupling, nor the right band-head energies. We may need to free V_q and V_s in order to improve this situation. We plan to calculate electromagnetic properties of the odd-odd Re in the near future. We also plan to extend the calculation to more neutron-deficient odd-odd Re nuclei.

a. KVI, Groningen

References

1. O. Scholten, K.V.I. Ann. Report, 1986.
2. O. Scholten, Ph.D. Thesis, University of Groningen, 1980.
3. C. Fahlander and G.D. Dracoulis, Nucl. Phys. A375, 263 (1982).
4. R. Hochel, P.J. Daly, and K.J. Hofstetter, Nucl. Phys. A211, 165 (1973).
5. M.R. Schmorak, Nucl. Data Sheet 13, 267 (1974).
6. M.V. Hoehn, E.B. Shera, Y. Yamazaki, and R.M. Steffen, Phys. Rev. Lett. 39, 1313 (1977).
7. S.A. Lane and J.X. Saladin, Phys. Rev. C6, 613 (1972).
8. P.P. Singh, L.R. Medsker, G.T. Emery, L.A. Beach and C.R. Gossett, Phys. Rev. C10, 656 (1974).
9. A. Artna-Cohen, Nucl. Data Sheet 16, 267 (1975).
10. C. Dors, F.M. Bernthal, and R.A. Warner, Cyclotron Laboratory, MSU, Ann. Report, 1973-1974.
11. I.M. Ladenbauer-Bellis, H. Bakhru, and P. Sen, Nucl. Phys. A252, 524 (1975).
12. M.F. Slaughter, R.A. Warner, T.L. Khoo, W.H. Kelly, and Wm.C. McHarris, Phys. Rev. C29, 114 (1984).

PREDICTION OF A NEW HIGH-SPIN MODE OF TRANSVERSE EXCITATION
IN ELECTRON SCATTERING FROM NUCLEI

B.A. Brown and B.H. Wildenthal^a

Modes of nuclear excitation which are mediated through a unique pair of shell-model orbitals are particularly interesting because of their freedom from the ambiguities which arise from interference between competing one-body transition paths. Such excitations yield direct insight into the many-nucleon structure of model wave functions and the global renormalization properties of the fundamental nuclear operators.

One example of such a unique-orbital excitation, which has been extensively studied, is the transverse magnetic mode, in which the total angular momentum transfer, ΔJ , has the maximum possible value for a given set of active single-particle orbitals. We will refer to this as the MJ_{\max} mode. In this mode, each member of the unique pair of orbitals has the maximum j -value, j_{\max} , for its major shell. Because these transitions are characterized by high angular momentum they stand out in spectra measured at large momentum transfers.

There are two classes of these MJ_{\max} excitations, one in which the two orbitals belong to the same major shell and the other in which the final j_{\max} belongs to a mostly unfilled major shell lying above the (mostly filled) major shell to which the the initial orbital belongs. Examples of the former are the "stretched" states observed in (p,n) reactions, such as the M7 in ^{48}Ca (p,n),¹ and the high-momentum transverse elastic electron scattering on odd-even nuclei, such as the M5 for ^{27}Al ,² and the M7 for ^{51}V .³ Examples of the latter are the "stretched" states seen in inelastic electron and hadron scattering,⁴ such as the M4 in ^{16}O ,⁵ the M6 in ^{28}Si ,⁶ the M8 in ^{48}Ca ,⁷ and ^{54}Fe ,⁸ and the M14 in ^{208}Pb .⁹

There is an analogous unique-orbital mode for transverse electric excitations which we

will refer to as the EJ_{\max} mode. This mode has received little theoretical or experimental attention. As we will see below, it is characterized by values of j_{\max} and $j_{\max}-1$ for the unique pair of orbitals. Of course, the formal existence of such a mode of excitation begs the question of whether it is manifested experimentally in concentrations of strength which are susceptible to measurement. Some evidence for the existence of this EJ_{\max} mode can be found in electron scattering to the 2^+ $T=1$ state at 16.11 MeV in ^{12}C ,¹⁰ which corresponds to the unique transition $0p_{3/2} \rightarrow 0p_{1/2}$, and to the 12^+ state at 6.10 MeV in ^{208}Pb ,⁶ which probably can be associated with the unique $0i_{13/2} \rightarrow 0i_{11/2}$ excitation.

We have made a thorough examination of the strength functions of all modes of longitudinal and transverse excitations which are predicted by the complete space sd-shell model wave functions of Wildenthal.¹² For nuclei near the center of the shell the spectra of transverse excitation strength shows striking peaks at high momentum transfers in the range of excitation energy between 7 and 15 MeV. Analysis of these peaks shows them to result from $0d_{5/2} \rightarrow 0d_{3/2}$ $E4$ transitions which exhaust significant fractions of the total strength available for this mode of excitation. The calculated transverse excitation functions for ^{26}Mg for three values of the momentum transfer are shown in Fig. 1. A strong state near 7.3 MeV in excitation energy, which appears to correspond to our prediction at this energy, has recently been discovered in the analysis of electron scattering data.¹³

For these strong transverse $E4$ states predicted by the shell model we find that the magnetization-current (MC) part of the TE operator makes the dominant contribution. The

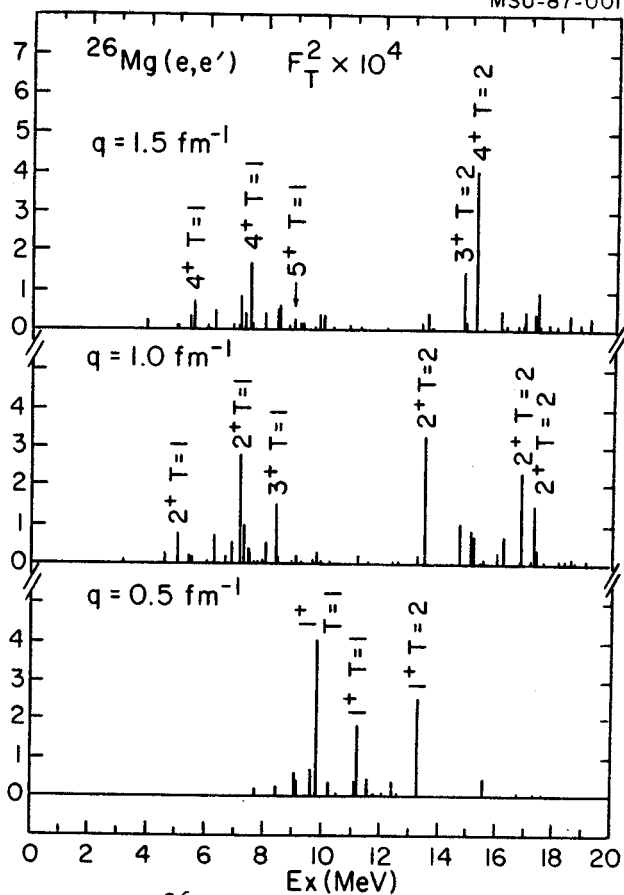


Fig. 1. The $^{26}\text{Mg}(e,e')$ transverse form factor plotted as a function of excitation energy for three values of the momentum transfer. The stronger states, as well as the strongest 5^+ state, are labeled by their J^π and isospin values.

convection-current contributions, which at low-momentum transfer can be related to the longitudinal form factor via the continuity equation (see section IV.E of Ref. 14), are very small in the higher momentum transfer region in which the MC contribution peaks. The reduced single-particle TE(MC) matrix element used in the plane-wave impulse approximation obeys the symmetry relation $\langle j || \text{TE(MC)} || j' \rangle = (-1)^{j-j'+1} \langle j' || \text{TE(MC)} || j \rangle$.¹⁴ As a consequence, the diagonal matrix elements ($j=j'$) of the TE(MC) operator vanish. Hence, the EJ_{max} form factors are dominated by transitions of the type $j_> = \ell+1/2 \rightarrow j_< = \ell-1/2$, with $J_{\text{max}} = j_> + j_< = 2\ell_{\text{max}}$, where ℓ_{max} is the largest value of the single-particle orbital angular momentum ℓ within a given major shell.

We note that M1 excitations also have a large $j_> + j_<$ component. However, the M1 mode is more complicated since $j_> \rightarrow j_>$ transitions are also allowed. For closed shell configurations in nuclei such as ^{208}Pb , these $j_> \rightarrow j_>$ components are completely blocked, but they enter with some strength from the non-closed shell components of the ground-state wave function. In contrast, these $j_> \rightarrow j_>$ components are never present for the EJ_{max} mode because of the selection rules associated with the operator.

The strengths of these EJ_{max} transitions are maximized by having the $j_>$ orbit filled and the $j_<$ orbit empty. In the sd shell this is realized in ^{28}Si . The strongest E4 we predict from the wave functions of Ref. 12 is for a T=1 state in ^{28}Si at 11.68 MeV excitation. The E4 form factor for this state peaks at $q = 1.65 \text{ fm}^{-1}$ (using harmonic-oscillator radial wave functions with $\hbar\omega = 12.4 \text{ MeV}$) and has a peak value of 0.7×10^{-4} (in the units defined in Ref. 14). This state exhausts about 60% of the total E4 (MC) strength in this nucleus. Due to ground-state configuration mixing in the full sd-shell wave function, the total strength predicted is about a factor of two smaller than that obtained with the zeroth-order, $(0d_{5/2})^{12}$, ground-state configuration.

This $4^+ T=1$ state in ^{28}Si is the analogue of the 4^+ state in ^{28}Al which lies experimentally at 2.27 MeV excitation.¹⁵ Thus, the experimental state should be at about 11.59 MeV excitation in ^{28}Si (i.e. 2.27 MeV above the known lowest T=1 state at 9.32 MeV). A state at this energy is seen in the $160^\circ (e,e')$ spectrum of Ref. 16, but the momentum transfer for this spectrum ($q = 1.9 \text{ fm}^{-1}$) is not optimum for E4. A state at 11.59 MeV has also been observed in inelastic pion scattering and assigned as a $6^- T=0$ state¹⁶ (a $6^- T=0$ state should be very weak in the electron scattering since isoscalar magnetic excitations are intrinsically a factor of $[(g_p - g_n)/(g_p + g_n)]^2 = 29$ weaker than isovector

transitions). Indeed, both of these states may be present at 11.59 MeV.

The E4 transitions are also strong in ^{26}Mg , see Fig. 1. Since the ground state of ^{26}Mg has $T=1$, the $\Delta T=1$ excitations are divided between the final states with $T=1$ and $T=2$. We predict the strongest states to lie at excitation energies of 7.41 MeV ($T=1$) and 15.14 MeV ($T=2$) with peak values of 0.18×10^{-4} and 0.42×10^{-4} , respectively. These states exhaust about 40% ($T=1$) and 70% ($T=2$) of the total calculated E4 strength. These total strengths amount to 50% of the total strength obtained with the zeroth-order $(0d_{5/2})^{10}$ ground-state configuration. The isospin splitting has brought the strength in the $T=1$ state down into a region of the spectrum in which any M4 and M6 excitations should be weak.

The experimental identification of the EJ_{max} excitation mode is not model independent. Using harmonic-oscillator radial wave functions, the E4 form factors are calculated to have exactly the same shape for the sd-shell configurations as M5 form factors. Thus, the shape cannot be used as a means of discriminating between these two modes. However, for the zeroth-order configurations [$(0d_{5/2})^{12}$ for ^{28}Si and $(0d_{5/2})^{10}$ for ^{26}Mg] M5 excitations are not allowed and even with the configuration mixed wave functions of Ref. 12 the calculated M5 strength is negligible compared to the E4 strength. (The strongest predicted M5 state for ^{26}Mg is labeled in Fig. 1.)

The strongest competing transitions likely to be observed experimentally in the transverse spectrum of ^{26}Mg arise from the cross-shell M4 and M6 excitations. The lowest and strongest 6^- (M6) $T=1$ state in ^{28}Si has been identified at 14.36 MeV in (e, e') .⁶ Based on a pure $0d_{5/2} \rightarrow 0f_{7/2}$ transition we calculate the M4 form factor to peak at $q = 1.27 \text{ fm}^{-1}$ and the M6 form factor to peak at $q = 1.82 \text{ fm}^{-1}$. Thus, from the position of the maximum one may qualitatively

discriminate these from the E4 excitations which peak at $q = 1.65 \text{ fm}^{-1}$.

Of course, an E4 state can be discriminated from M4, M5 and M6 states by the fact that the E4 can contain a longitudinal (C4) component, whereas for the ML transitions the longitudinal components must vanish. For the state at 11.68 MeV in ^{28}Si , we calculate a longitudinal form factor which peaks at $q = 1.5 \text{ fm}^{-1}$ with a value of 0.17×10^{-3} (again in the units of Ref. 14). However, there is probably some uncertainty in this calculated value since it is relatively weak compared to the strong C4 transitions for 4^+ states at low excitation.¹⁷

It is interesting to note that the state at 7.41 MeV in ^{26}Mg is the sixth 4^+ state predicted in the shell model spectrum. Many of the lower states have been studied previously in (e, e') experiments, being observed through their strong C4 components.¹⁸ The calculated C4 form factor for the 7.41 MeV state has a peak value of 0.8×10^{-4} ; however, again we note that because of its relatively small magnitude this value is somewhat uncertain.

Several additional experiments are suggested by our analysis. This EJ_{max} mode may be selectively excited by other probes such as pions and protons. However, we note that these normal-parity EJ-type transitions are relatively weak in (p, n) reactions with E_p in the range of 100-200 MeV.¹⁹ It would be interesting to look for stretched EJ transition in other nuclei. The E4 in ^{28}Si and the E6 in nuclei around the ^{48}Ca and ^{56}Ni closed shells would be good candidates.

a. Drexel University, Philadelphia, PA.

References

1. B.D. Anderson, T. Chittrakarn, A.R. Baldwin, C. Lebo, R. Madey, R.J. McCarthy, J.W. Watson, B.A. Brown, and C.C. Foster, Phys. Rev. C31, 1147(1985).

2. T.W. Donnelly and I. Sick, Rev. Mod. Phys. 56,461(1984).
3. P.K. A. de Witt Huberts, L. Lapikas, H. Deries, J.B. Bellicard, J.M. Cavedon, B. Frois; M. Huet, Ph. Leconte, A. Nakada, Phan Xuan Ho, S.K. Platchkov and I. Sick, Phys. Lett. 71B,317(1977).
4. R.A. Lindgren, M. Leuschner, B.L. Clausen, R.J. Peterson, M.A. Plum and F. Petrovich, in Nuclear Structure at High Spin, Excitation and Momentum Transfer, Indiana Univ. 1985, ed. by H. Nann (AIP Conference Proceedings 142, 1986), p.133.
5. I. Sick, E.B. Hughes, T.W. Donnelly, J.D. Walecka and G.E. Walker, Phys. Rev. Lett. 23,1117(1969).
6. S. Yen, R. Sobie, H. Zarek, B.O. Pich, T. E. Drake, C.F. Williamson, S. Kowalski and C.P. Sargent, Phys. Lett. 93B,250(1980).
7. J.E. Wise, J.S. McCarthy, R. Altemus, B.E. Norum, R.R. Whitney, J. Heisenberg, J. Dawson and O. Schwentker, Phys. Rev. C31, 1699(1985).
8. R.A. Lindgren, J.B. Flanz, R.S. Hicks, B. Parker, G.A. Peterson, R.D. Lawson, W. Teeters, C.F. Williamson, S. Kowalski and X.K. Maruyama, Phys. Rev. Lett. 46,706 (1981).
9. J. Lichtenstadt, J. Heisenberg, C.N. Papanicolas, C.P. Sargent, A.N. Courtemanche and J.S. McCarthy, Phys. Rev. C20,497(1979).
10. J.B. Flanz, R.S. Hicks, R.A. Lindgren, G.A. Peterson, A. Hotta and R.C. York, Phys. Rev. Lett. 41,1642(1978).
11. J. Lichtenstadt, C.N. Papanicolas, C.P. Sargent, J. Heisenberg and J.S. McCarthy, Phys. Rev. Lett. 44,858(1980).
12. B.H. Wildenthal, Progress in Particle and Nuclear Physics, (Pergamon Press, 1983) Vol. 11, p. 5.
13. K.K. Seth, private communication.
14. B.A. Brown, B.H. Wildenthal, C.F. Williamson, F.N. Rad, S. Kowalski, H. Crannell and J.T. O'Brien, Phys. Rev. C32, 1127(1985) and references therein.
15. C.M. Lederer and V.S. Shirley, Table of Isotopes, (John Wiley and Sons, 1978).
16. C. Olmer, B. Zeidman, D.F. Geesaman, T.S.H. Lee, R.E. Segel, L.W. Swenson, R.L. Boudrie, G.S. Blanpied, H.A. Thiessen, C.L. Morris and R.E. Anderson, Phys. Rev. Lett. 43,612(1979).
17. B.A. Brown, R. Radhi and B.H. Wildenthal, Physics Reports 101,314(1983).
18. E.W. Lees, A. Johnston, S.W. Brain, C.S. Curran, W.A. Gillespie and R.P. Singhal, J. Phys. G7,936(1974).
19. B.D. Anderson, C. Lebo, A.R. Baldwin, T. Chittrakarn, R. Madey, J.W. Watson, and C.C. Foster Phys. Rev. Lett. 52,1872 (1984).

B.A. Brown and W.A. Richter^a

The best available two-body effective interactions are obtained using an unconstrained Hamiltonian, i.e. all two-body matrix elements and single-particle energies are allowed to vary as free parameters in a fit to experimental data. In the most comprehensive work of this type, for example, Wildenthal¹ has been able to reproduce a selection of 447 s-d shell binding and excitation energies with an rms deviation between experiment and theory of about 150 keV. However, such parameters generally reveal very little about the nature or form of the nucleon-nucleon interaction. It is also much more difficult to extract an unconstrained Hamiltonian from fits in spaces larger than the s-d shell, due to the large number of two-body matrix elements on the one hand, and a lack of sufficient data on the other. Hence, the goals of our work have been:

- 1) to systematically explore the types of constraints which can be placed on the s-d shell two-body interaction when based on general forms expected from one-boson exchange type potentials (OBEP),
- 2) to apply these constraints so as to achieve a fit to the s-d shell data that is comparable to that obtained with a purely empirical interaction, and
- 3) to extend the method to obtain an improved Hamiltonian for larger model spaces, such as the f-p shell.

The important physical aspects of the residual interaction can be more readily discerned by transforming the representation of the two-body matrix elements from the j-j coupling scheme (which is the representation generally needed for shell-model calculations) to the L-S coupling scheme, and following this by a spin-tensor decomposition of these

elements. This technique has recently been applied² to the original 63 j-j coupled empirical two-body matrix elements in the s-d shell referred to above, and is used throughout our work to assess the relative importance of the various spin-tensor components of different interactions.

A variety of forms for the two-body interaction with strengths adjusted to fit experimental energies have been considered. The general central part has been compared with those obtained from schematic interactions such as the delta, modified surface delta, monopole-monopole and Q.Q. For our proposed interaction we started with a convenient parameterized form of G-matrix elements based on finite range one-boson (OBEP) exchange potentials, in which the oscillator bare G-matrix elements of the Reid and Paris potentials have been fitted to the OBEP oscillator matrix elements.³ The G-matrix was then modified, by adding correction terms for core-polarization and density-dependence. The core-polarization contribution to the interaction was parameterized in terms of multipole-multipole interactions.

By basing the Hamiltonian on a bare G-matrix plus corrections terms and doing a spin-tensor decomposition, those components which are most important in determining shell-model eigenvalues could be adjusted to their optimum values relative to experimental energies, and those elements to which the shell-model eigenvalues are quite insensitive could be held fixed. The adjustments obtained in such fits yield optimal corrections introduced by approximations made in calculating the G-matrix. These empirical modifications have been compared to those expected from core polarization and other nuclear medium modifications.

Extensive fits using various combinations of parameters have been made to the same basic energy data set of Ref. 1, followed by an analysis of the resulting two-body matrix elements into central, spin-orbit, tensor and antisymmetric spin-orbit components.⁴ The latter were found to be the least important, and as these components were not well determined from the fits, they were set equal to zero.

The analysis favors a density-dependent form for the central and spin-orbit components. We developed an empirical "best-fit" interaction containing 14 two-body parameters which is able to reproduce 447 sd-shell energy-level data to within an rms deviation between experiment and theory of about 250 keV.⁴

For an example we show the experimental energy levels of ²²Na compared to those calculated with the new 14-parameter interaction in the middle of Fig. 1 (Th-B). This is compared with two other results; on the left-hand side (Th-A) a "no-parameter" calculation based on the Paris potential G matrix,⁵ and on the right-hand side (Th-C) a calculation based on Wildenthal's completely empirical (66-parameter) two-body matrix elements.

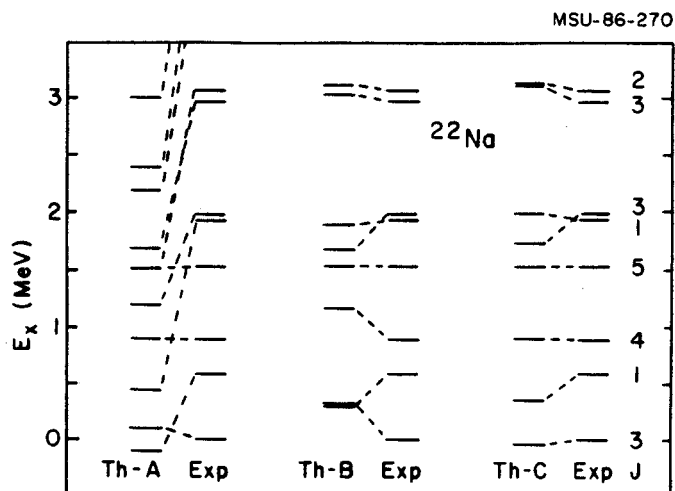


Fig. 1. Low-lying excited states of ²²Na compared with three theoretical calculations discussed in the text.

We propose to use this modified G-matrix interaction as a starting point for the effective interaction in other mass regions, in

particular, for the fp shell. Some preliminary fits have already been carried out in the full f-p shell for A = 41-46 nuclei,⁶ and the quality of fits obtained are encouraging. At present we are engaged in iterating the fitting procedure by recalculating the one- and two-body transition densities at each stage using the OXBASH shell-model code. In addition to the VAX-780 we are looking into using faster computers.

Future work in this area will be concerned with studying the relationship between parameters in different model spaces. We would also like to study a wider range of observables, including total-binding energies, single-particle energies, and the two-particle spectra of nuclei near the closed-shell nuclei up to ²⁰⁸Pb.

a. University of Stellenbosch, South Africa.

References

1. B. H. Wildenthal, Progress in Particle and Nuclear Physics, Vol 11, edited by D. H. Wilkinson (Pergamon Press, Oxford), p.5.
2. B. A. Brown, W. A. Richter and B. H. Wildenthal, J. Phys. G11,1191(1985).
3. A. Hosaka, K. I. Kubo and H. Toki, Nucl. Phys. A444,76(1985).
4. B. A. Brown, W. A. Richter, R. E. Julies and B. H. Wildenthal, unpublished; B. A. Brown: Achievements and Goals of Recent Shell-Model Calculations. Invited talk presented at the International Nuclear Physics Conference, Harrogate, U.K., 25-30 August 1986.
5. J. Shurpin, T. T. S. Kuo and D. Strottman, Nucl. Phys. A408,310(1983).
6. B. A. Brown, W. A. Richter, M. G. Van der Merwe, R. E. Julies, unpublished.